energies

MDPI

Article

The Application of Water Cycle Optimization Algorithm for Optimal Placement of Wind Turbines in Wind Farms

Hegazy Rezk [1,2,*], Ahmed Fathy [3,4], Ahmed A. Zaki Diab [2] and Mujahed Al-Dhaifallah [5,*]

1 College of Engineering at Wadi Addawaser, Prince Sattam Bin Abdulaziz University, Al-Kharj 11991, Saudi Arabia
2 Electrical Engineering Department, Faculty of Engineering, Minia University, Al Minya 61519, Egypt; ahmed.zaki.diab@mu.edu.eg
3 Electrical Engineering Department, Faculty of Engineering, Jouf University, Sakakah 42421, Saudi Arabia; afali@zu.edu.eg
4 Electrical Power and Machine Department, Faculty of Engineering, Zagazig University, Zagazig 44519, Egypt
5 Systems Engineering Department, King Fahd University of Petroleum and Minerals, Dhahran 31261, Saudi Arabia
* Correspondence: hegazy.hussien@mu.edu.eg (H.R.); mujahed@kfupm.edu.sa (M.A.-D.)

Received: 8 October 2019; Accepted: 13 November 2019; Published: 14 November 2019

Abstract: Wind farms (WFs) include an enormous number of wind turbines (WTs) in order to achieve high capacity. The interaction among WTs reduces the extracted amount of wind energy because wind speed decreases in the wake region. The optimal placement of WTs within a WF is therefore vital for achieving high performance. This permits as many WTs as possible to be installed inside a narrow region. In this work, the water cycle algorithm (WCA), a recently developed optimizer, was employed to identify the optimal distribution of WTs. Minimization of the total cost per kilowatt was the objective of the optimization process. Two different cases were considered: the first assumed constant wind speed with variable wind direction, while the second applied variable wind speed with variable wind direction. The results obtained through the WCA optimizer were compared with other algorithms, namely, salp swarm algorithm (SSA), satin bowerbird optimization (SBO), grey wolf optimizer (GWO), and differential evolution (DE), as well as other reported works. WCA gave the best solution compared to other reported and programmed algorithms, thus confirming the reliability and validity of WCA in optimally configuring turbines in a wind farm for both the studied cases.

Keywords: modern optimization; wind farm; energy efficiency; optimal placement

1. Introduction

A sharp increase in the demand for electrical energy can be explained by a rapid increase in the human population. Electrical generation through renewable energy, namely, solar and wind, is becoming a popular and promising technology option. Renewable energy sources are being used in the field to minimize the dependence on traditional energy sources because of several benefits, such as the low amount of carbon and harmful gas emissions from renewable sources. Renewable energy is also clean, inconsumable, and abundant [1–4]. Therefore, securing electrical energy with minimum cost and no environmental impact is a goal worldwide. Wind energy systems (WES) have gained considerable attention as a green energy source as they are available in enormous amounts [5]. By the end of 2017, the total worldwide capacity of WES had increased by around 11% compared to 2016, reaching 539 GW. This was achieved by the addition of around 52 GW during 2017 [6]. Figure 1 shows the total capacity of WES around the world from 2007 to 2017. The top 10 countries with the largest

capacity of WES are shown in Figure 2. It can be seen that China, United States, and Germany are the top three countries in terms of WES capacity, contributing 19.7, 7, and 6.1 GW in 2017, respectively. In China, the contribution of WES in the total energy production has steadily increased in recent years, reaching 4.8% by the end of 2017 (up from 4% in 2016 and 3.3% in 2015) [6]. For large-scale electrical energy generation-based wind energy, an enormous number of WTs should be installed within a wind farm (WF).

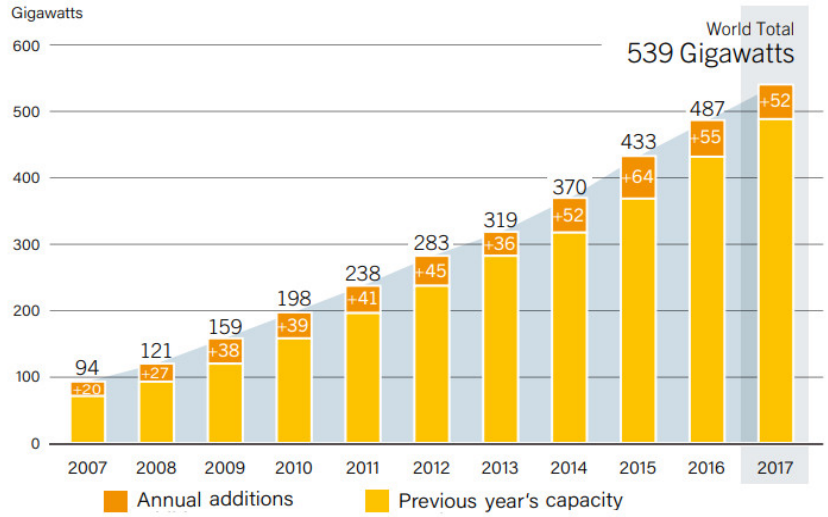

Figure 1. The total capacity of wind energy systems (WES) around the world from 2007 to 2017.

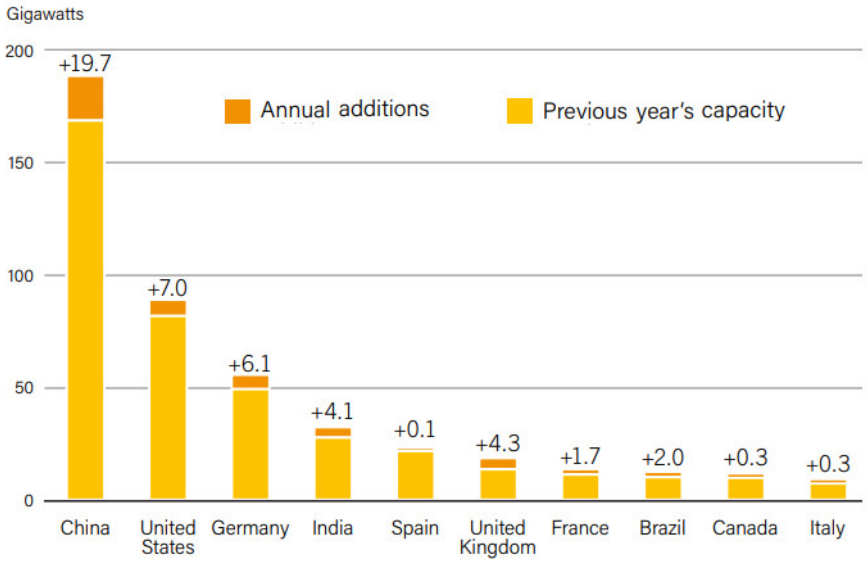

Figure 2. The top 10 countries that have the highest capacity of WES (figures for 2017).

The optimal distribution of wind turbines (WTs) plays a significant role in the design of WFs. A nonoptimal WF design leads to the negative effect of reducing harvested electrical energy due to the wake effect [7]. Such an effect is created by upstream WTs, which leads to a reduction in the speed of downstream WTs. Consequently, the harvested energy produced by downstream WTs is reduced compared to upstream WTs. Because the traditional layout of WTs significantly increases the wake effect, the optimal placement of WTs inside a WF can be considered as a good solution for reducing the wake effect in addition to improving the performance of the WF by increasing the harvested energy from WTs. Accordingly, the best distribution of WTs has gained considerable attention from

researchers in order to extract maximum harvested electrical energy from WFs with lower cost of energy per kilowatt.

Many previous works have sought to identify the optimal distribution of WTs within a WF [8–21]. The summary of these related works is presented in Table 1.

Table 1. Summary of previously reported studies.

Author	Year	Optimizer	Remarks
Khanali [8]	2018	Genetic algorithms	Actual wind speed data of Tehran were considered. The main finding was that the longitudinal space among WTs must be larger than the latitudinal distance in order to increase WF performance. The efficiency of WF was 89.5%.
Biswas [9]	2017	Differential evolution algorithm	The fitness function was the maximization of system efficiency. The decision variables were rotor diameters and hub heights.
Bryony [10]	2016	Pattern search algorithm	Two different cases of wind were considered: (1) constant value and direction and (2) three different values and directions.
Grady [11]	2005	Genetic algorithms	The two-dimensional Park model proposed by Jensen was used. The total cost of WF was minimized and at the same time the harvested energy was maximized.
Emami [12]	2010	Genetic algorithms	The capital cost of WF was considered as objective function.
Chen [13]	2013	Genetic algorithm	WTs with different hub heights were considered. The main conclusion was that employing WTs with different hub heights can increase power output in small WFs. Different cost models were considered.
Shakoor [14]	2014	Genetic algorithm	The linear Jensen's wake model was employed with definite selection criteria.
Turner [15]	2014	New mathematical programming	Both linear and quadratic formulas for optimization were considered.
Gao [16]	2015	Multipopulation genetic algorithm	Real data from offshore Hong Kong was collected. The WF performance was improved.
Eroğlu [17]	2012	Ant colony optimization (ACO)	The study showed that employing ACO can help improve the performance of WFs.
Chowdhury [18]	2012	Particle swarm optimization	The presented approach was not applied on a large scale. The work presented an experimental prototype.
Feng [19]	2015	Random search algorithm	The proposed strategy was found to be useful for WFs that had a constant number of WTs.
Marmidis [20]	2008	Monte Carlo simulation	A small-scale wind farm was used as case study. The results did not depend on real data.
Mora et al. [21]	2007	Evolutionary algorithm	The capital investment of WF was considered. Different economic factors were also considered.

Despite the advantages of different optimization algorithms reported in the literature, it has been proven by the "no free lunch" theorem [22] that no single algorithm is fit to deal with all different optimization problems. Such an assumption reveals the importance of new optimizers in different fields because the capability of an optimizer to solve a series of problems does not assure its effectiveness in other problems [23]. Some of the recently developed optimizers, such as water cycle algorithm (WCA) [24], salp swarm algorithm (SSA) [25], satin bowerbird optimization (SBO) [26], and grey wolf

optimizer (GWO), have not been employed in the process of optimal placement of WTs within a WF. This prompted the authors of the present paper to use them to determine the optimal distribution of WTs. The main aim was to optimize the position of WTs inside a WF in order to minimize the total cost per kilowatt. Two cases were studied: the first assumed constant wind speed with variable wind direction (CSVD), while the second applied variable wind speed with variable wind direction (VSVD). The results obtained were then compared with other reported works. The rest of the paper is structured as follows. Section 2 introduces the problem formulation. A brief overview of modern optimization algorithms is reviewed in Section 3. Section 4 presents and discusses the results. Finally, the conclusion is presented in Section 5.

2. Problem Formulation

The wind farm problem formulation included the following: wake model, harvested power model, wind farm efficiency model, cost model, and objective function. These are explained below.

2.1. Wake Model

The wake model of wind behavior is presented in [12]. Figure 3 illustrates the wake model, in which the k-th WT operates under the effect of a single turbine at the m-th location. The wind velocity of a downstream WT can be expressed by the following formula:

$$u_k = u_{0k}\left[1 - \frac{2a}{\left(1 + a_m\left(\frac{x_{mk}}{r_{m1}}\right)\right)}\right] \tag{1}$$

where u_k is the downstream WT wind velocity, u_{0k} is the free flow velocity at the k-th WT with no wake effect, x_{mk} is the space from the upstream turbine (between the m-th and the k-th turbine), a denotes the axial induction factor, α_m is the entrainment constant, and r_{m1} is the rotor radius of the m-th downstream turbine. Moreover, r_{m1} can be calculated as a function of the turbine radius r_m as follows [12]:

$$r_{m1} = r_m\sqrt{\frac{1-a}{1-2a}} \tag{2}$$

where the axial induction factor a is calculated as follows:

$$a = \frac{1 - \sqrt{1 - C_T}}{2}.$$

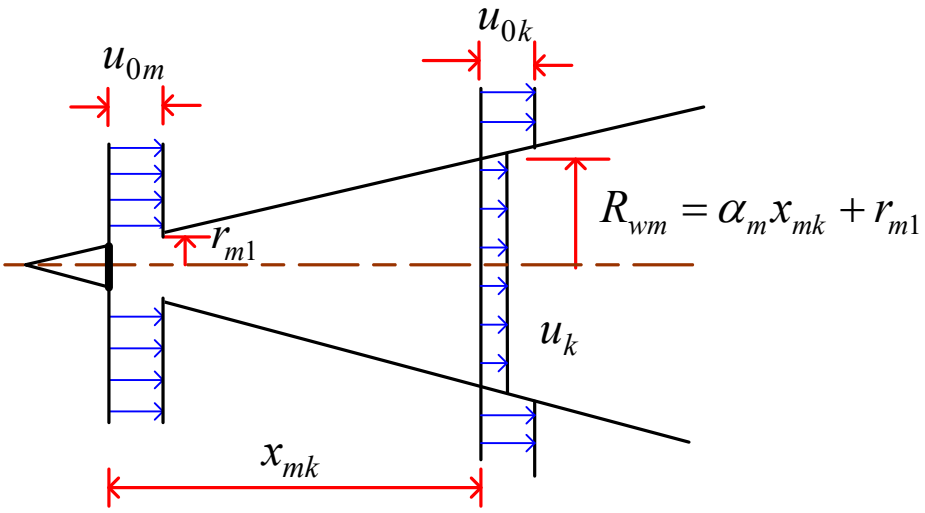

Figure 3. Wake model by Jensen.

Furthermore, the turbine thrust coefficient C_T can be estimated as follows [9]:

$$C_T = 4\alpha_m(1-\alpha_m) \tag{3}$$

where α_m is the entrainment constant [9]:

$$\alpha_m = \frac{0.5}{\ln(\frac{h_m}{z_0})} \tag{4}$$

where h_m is the m-th turbine hub height, and z_0 is the roughness of the terrain surface. In the linear wake model, the wake region is represented in conical form with a radius written as follows:

$$R_{wm} = \alpha_m x_{mk} + r_{m1} \tag{5}$$

At the k-th WT, the wind speed is a function of the WT hub height as follows:

$$u_{0k} = u_{ref}\log(\frac{h_k}{z_0})/\log(\frac{h_{ref}}{z_0}). \tag{6}$$

In this work, the reference hub height and the corresponding wind speed were considered as h_{ref} = 60 m and u_{ref} = 12 m/s, respectively, with z_0 being 0.3 [9].

In the zone inside various wake flows, the velocity deficit may be improved. If the i-th WT is considered under the effect of various wake flows with consideration of the superimposed influence of wake flow, the wind speed at the position of the i-th WT can be calculated as follows [12]:

$$u_i = u_{0i}\left[1 - \sqrt{\sum_{j=1}^{N_T}\left(1-\frac{u_{ij}}{u_{0j}}\right)^2}\right] \tag{7}$$

where u_{0i} and u_{0j} denote the local wind speeds with no wake effect, u_{ij} is the wind speed at the i-th WT under the effect of the j-th turbine, and N_T denotes the number of WTs affecting the i-th WT with wake effects. A constrained variation in the rotor diameters and hub heights is assumed. Moreover, the downstream WT is distant enough for the full wake influence to be considered instead of the partial wake influence generated via the upstream turbine.

2.2. Harvested Power Model

The layout used in [10] for the study of constant wind speed and fixed wind direction was reconsidered in the present work. In the case of constant rotor radius, the total power extracted from each turbine can be calculated as $P_i = 0.3u^3$, with 20 m considered as the rotor radius. Because the radius of a WT rotor is variable, the constant factor cannot be approximated. Therefore, the power equation can be expressed as follows:

$$P_i = 0.5\rho\pi r^2 u^3 C_p/1000 \text{ kW} \tag{8}$$

where ρ is the density of the air, and C_p is the efficiency of the rotor.

2.3. WF Efficiency Model

After estimating the power of each WT in the WF inside the wake, the total extracted power from the WF can be expressed as follows:

$$P_{WF} = \sum_{i=1}^{N} P_i \tag{9}$$

The maximum output power from the WF neglecting the wake influence can be calculated as follows:

$$P_{WF,\max} = \sum_{i=1}^{N} P_{i,\max} \tag{10}$$

where $P_{i,\max}$ is the maximum output power from the turbine neglecting the wake influence.

Thus, the efficiency of the WF can be expressed by the following equation:

$$\eta = \frac{P_{WF}}{P_{WF,\max}} \tag{11}$$

2.4. Normalized Cost Model

Mosetti [27] proposed a normalized cost equation of WF installation based on only the total number of turbines. This equation is the basic model that has been used for evaluating the cost of WF installation in most previous works. The nondimensionalized number of cost/year for WT is assumed as 1. Moreover, the maximum cost will be reduced by 1/3 for each turbine if the number of WTs is large. Consequently, the normalized cost of WF installation may be formulated as follows:

$$\text{cost}_{\text{Normalized}} = N\left(\frac{2}{3} + \frac{1}{3}e^{-0.00174N^2}\right) \tag{12}$$

The cost model can be modified and rewritten by considering the variation in the rotor diameter and the hub height as follows [9]:

$$Cost = \text{cost}_{\text{Normalized}}\left(1 + \frac{1}{N}\sum_{i=1}^{v1} 0.0039825 x_i N_i + \frac{1}{N}\sum_{j=1}^{v_2} 0.0016425 x_j N_j\right) \tag{13}$$

where $\text{cost}_{\text{Normalized}}$ is the base cost at the base radius of 20 m and base height of 60 m, x_i is the rotor radius variation at the i-th turbine, x_j is the hub height variation of the i-th turbine, v_1 is the number of turbines that have different rotor radii, v_2 is the number of turbines with different hub heights, N_i is the number of i-th turbines with different rotor radii, N_j is the number of j-th turbines with different hub heights, and N is the number of WTs.

2.5. Objective Function

In this work, the objective function was set as the cost/kilowatt of generated power, and it can be calculated as follows:

$$obj.function = \frac{\cos t}{\sum_{i=1}^{N} P_i} \tag{14}$$

Figure 4 shows a flowchart illustrating the application of optimization algorithms to solve and optimize the optimal placement of WTs within a WF. The procedure employed in the present work was as follows. The first step involved initializing the wind turbine data by defining the WF boundaries. After that, the wake effect was investigated for each WT, and the local velocity of each one was determined. The proposed objective function, i.e., the cost per kilowatt power, was then calculated based on the current layout of the WTs. Next, the end criteria were investigated, and the presented optimization approach was applied to obtain a new WT layout that would minimize the total cost per kilowatt. These steps were repeated until the optimal layout was achieved.

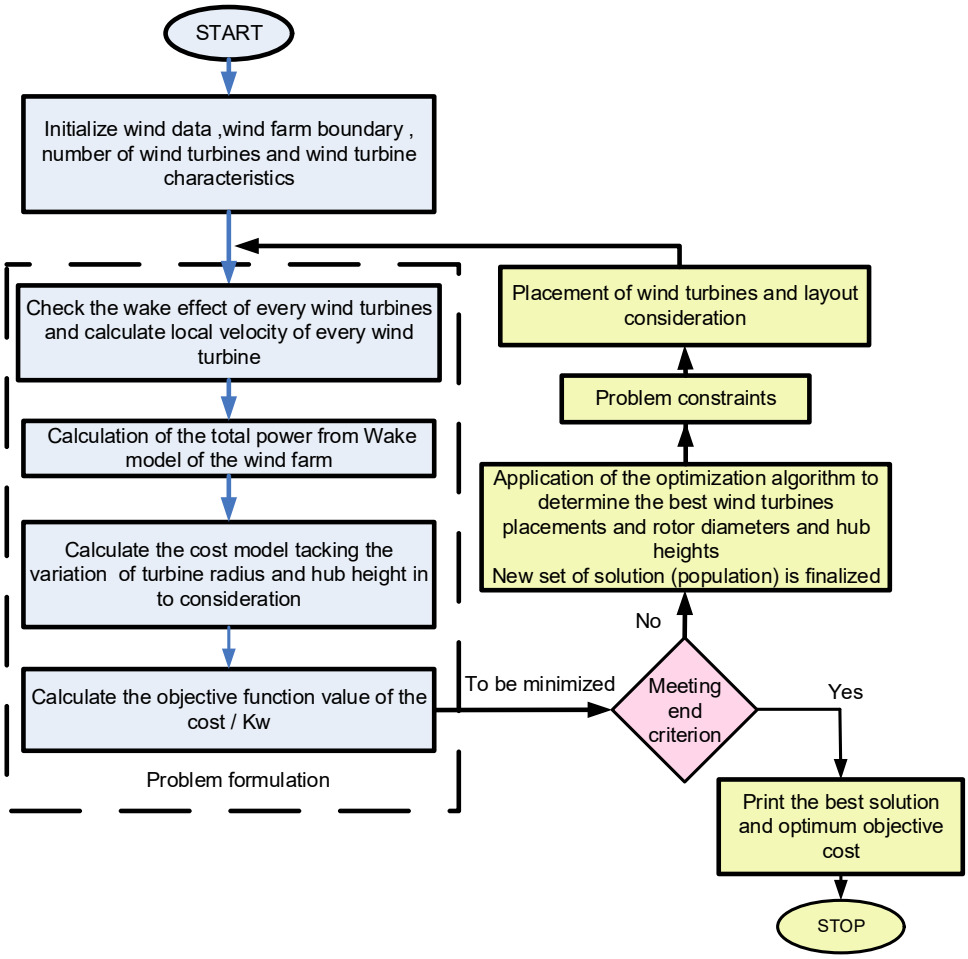

Figure 4. Process of optimal placement of wind turbines (WTs) within a wind farm (WF).

3. Brief Overview of Modern Optimization Algorithms

3.1. Water Cycle Algorithm

The WCA was proposed by Eskandar [24]. The core idea of WCA is extracted from water moving below or above the Earth's surface. Generally, streams influx into rivers, and rivers influx into the sea. The main advantage of WCA is that it only has a few number of tuning parameters. The initial population is selected in a random way after a rain event. The sea is selected as the best individual, the river is considered as a number of good individuals, and the rest represents the stream [24]. The streams are generated from rain drops, which form a river after joining each other. Additionally, some streams outflow directly into the sea, which is considered as the optimal solution. Figure 5 explains the movement of streams toward a specific river through a line of distance d. A similar idea can also be used for river fluxing to the sea.

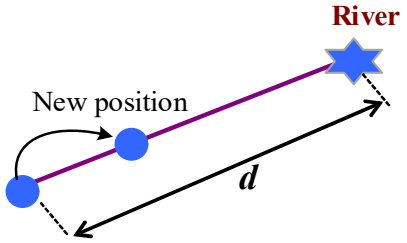

Figure 5. Stream's movement toward the river.

The stream and river positions can be estimated using Equations (15) and (16), respectively [24,28]:

$$x_{Stream}^{t+1} = x_{Stream}^{t} + rand \times C \times \left(x_{River}^{t} - x_{Stream}^{t}\right) \quad (15)$$

$$x_{River}^{t+1} = x_{River}^{t} + rand \times C \times \left(x_{Sea}^{t} - x_{River}^{t}\right) \quad (16)$$

where $x_{Stream}{}^{t}$, $x_{River}{}^{t}$, and $x_{Sea}{}^{t}$ are the stream, river, and sea positions at the t-th iteration, respectively, and *rand* is a random value in the range [0, 1]; C is selected as 2.

3.2. Salp Swarm Algorithm

SSA a modern metaheuristic algorithms that was introduced in 2017 by Mirjalil [25]. Salps are members of the Salpidae family and have diaphanous cylinder bodies; they are similar in movement and tissues to jelly fish. Water is pumped through the body as propulsion for the salps to move forward. The shape of an individual salp and a swarm of salps, which is also called salp chains, is shown in Figure 6.

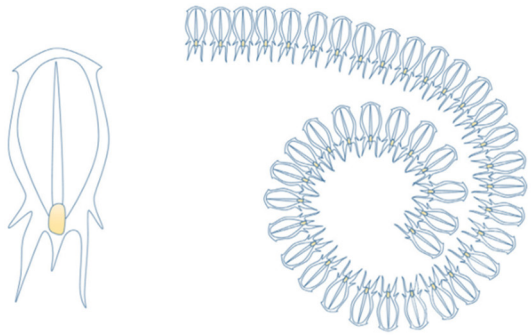

Figure 6. Individual salp and swarm of salps.

A string of salps attempts to detect a better location of food source through a screening procedure assisted by the chief salp; the remainder salps are followers. Similar to differential evolution (DE) techniques, the particle position in the search area is explained with the nPop × nDim matrix, where nPop denotes the number of salps, and nDim denotes the number of dimensions. The number of salps is selected based on the user, whereas the number of dimensions relies on the number of variables that require optimization. Next, each salp location is modified based on information received from the chief salp to swallow the best food [25]. The position of the leader is updated according to the food position as follows:

$$x_j^1 = \begin{cases} F_j + r_1\left(\left(ub_j - lb_i\right)r_2 + lb_i\right) & r_3 \geq 0 \\ F_j + r_1\left(\left(ub_j - lb_i\right)r_2 + lb_j\right) & r_3 < 0 \end{cases} \quad (17)$$

where $x_j{}^1$ is the leader's position in the j-th dimension; Fj is the place of food source in the j-th dimension; ub_j and lb_j are the upper and lower bounds of the j-th dimension, respectively; r_1, r_2, and r_3 are numbers with random value. The coefficient r_1 is considered as the effective parameter in salp swarm algorithm due to its role in maintaining a balance between the exploration and exploitation stages [25]. Equation (18) shows how to mathematically determine the value of this coefficient:

$$r_1 = 2e^{-\left(\frac{4t}{T}\right)^2} \quad (18)$$

where t indicates the present iteration, and T is the total number of iterations. The parameter r_2 and r_3 are random numbers that have value between [0, 1]. The follower's location is updated based on the following equation [25]:

$$Y_j{}^i = 0.5at^2 + v_0 \quad (19)$$

where t is the time, v_0 is the initial speed, and a is the ratio between the initial and final speeds. The rate of discrepancy among iterations is considered as 1, and v_0 is equal to zero. Due to the optimization time in the iteration, Equation (19) can be expressed as follows:

$$Y_j^i = 0.5\left(Y_j^i + Y_j^{i-1}\right) \tag{20}$$

The main steps of the SSA optimizer are explained in Figure 7 [29]. The optimizer starts the process by setting a random position for each salp. Then, it estimates the cost function for each salp, finds out the leader salp that has the maximum fitness, and assigns the position of the leader salp as the food source to be chased by the salp string. Next, the new positions for salps are modified. If any of the salps exceeded the search space, it will be recovered on the boundaries. This process is continued until the end criteria are achieved.

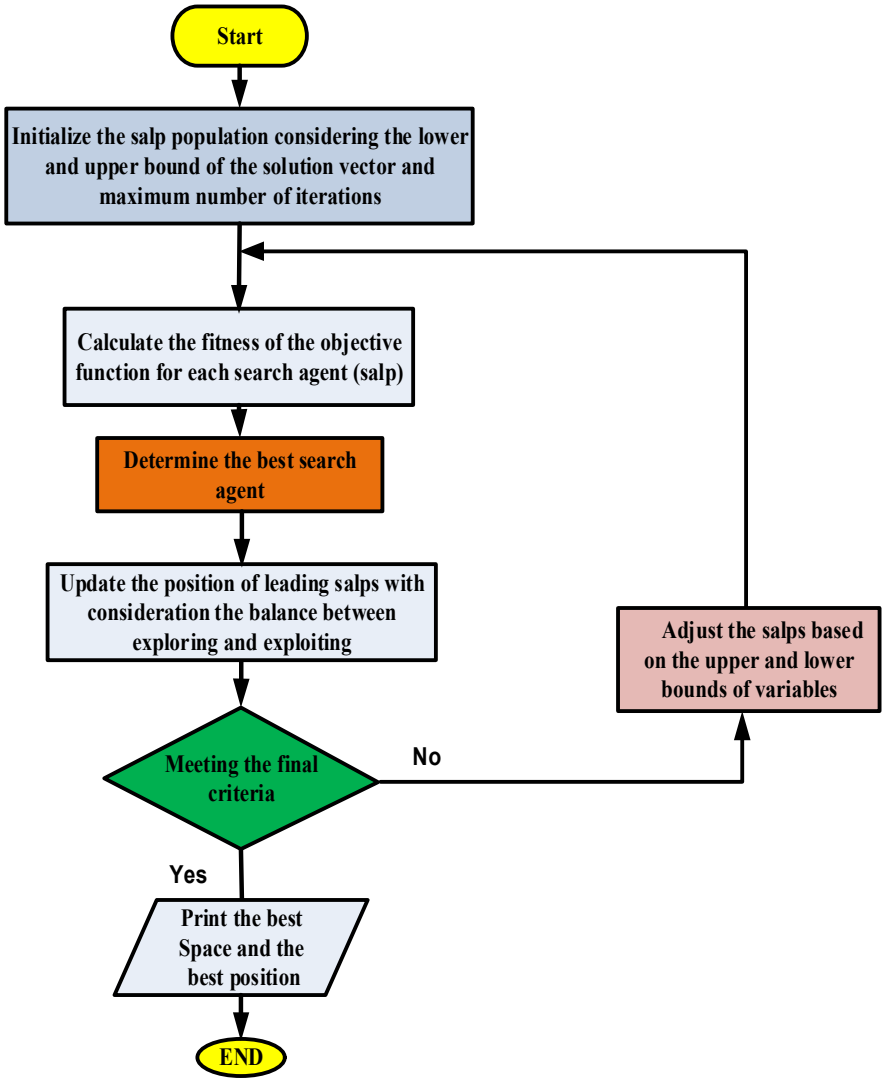

Figure 7. Salp swarm algorithm (SSA) optimization process.

3.3. Satin Bowerbird Optimization

Satin bowerbirds live inside Australian rainforests. Throughout the autumn and winter seasons, bowerbirds disuse their own locations and stir to open woodlands to devour fruits and pests. However, during the breeding period, bowerbirds drove together in little groups, inhabiting territories that they clearly inhabit year after year [26,30]. According to the SBO technique, adults build up a trellis with

various materials on the ground during the mating period. Based on the moralities of a bowerbird's life, the SBO approach is applied to update the new position as follows [26,30]:

$$x_{ik}^{new} = x_{ik}^{old} + \lambda_k \left(\left(\frac{x_{jk} + x_{elite,k}}{2} \right) - x_{ik}^{old} \right) \tag{21}$$

where x_i denotes the i-th vector of the solution, x_{ik} is the k-th member, x_j is the target solution in the current iteration, x_{elite} denotes the position of the elite, and λ_k determines the bower's attraction power.

3.4. Grey Wolf Optimizer

The GWO is considered as a modern metaheuristic algorithm that is utilized for optimization of nonlinear problems. GWO was introduced by Mirjalili, and it simulates the social hierarchy and hunting mechanism of grey wolves [31]. Generally, GWO contains three phases: searching for prey, encircling prey, and attacking prey. Grey wolves are segmented into four levels. The best level of solution is called alpha (α) wolf. The second and third solutions are named beta (β) and delta (δ) wolves, respectively. The last level of solution is omega (ω) wolf, which is deemed as the lowest degree in grey wolves.

During the hunting period, grey wolves surround the prey, and the behavior of encircling can be represented by the following equations [31,32]:

$$\vec{D} = \left| \vec{C} \vec{X}_p(t) - \vec{X}(t) \right| \tag{22}$$

$$\vec{X}(t+1) = \vec{X}_p(t) - \vec{A}\vec{D} \tag{23}$$

where t is the current position, $\vec{X}_p$ is the vector of the prey's position, $\vec{X}$ is the vector of the position of grey wolves, $\vec{A}$ and $\vec{C}$ indicate the coefficient vectors, which are calculated as follows [31,32]:

$$\vec{A} = 2\vec{a}\vec{r}_1 - \vec{a} \tag{24}$$

$$\vec{C} = 2\vec{r}_2 \tag{25}$$

where $\vec{r}_1$ and $\vec{r}_2$ are random vectors and magnitude in the period [0, 1], $\vec{a}$ is the component vector, which decreases from 2 to 0. More details about the mathematical representation of the GWO process can be found in [32]. Agents modify their positions according to the position of the best search agent as follows:

$$\begin{aligned} \vec{D}_\alpha &= \left| \vec{C}\vec{X}_\alpha - \vec{X} \right| \\ \vec{D}_\beta &= \left| \vec{C}\vec{X}_\beta - \vec{X} \right| \\ \vec{D}_\delta &= \left| \vec{C}\vec{X}_\delta - \vec{X} \right| \\ \vec{X}_1 &= \left| \vec{X}_\alpha - \vec{A}_1\vec{D}_\alpha \right| \\ \vec{X}_2 &= \left| \vec{X}_\beta - \vec{A}_2\vec{D}_\beta \right| \\ \vec{X}_3 &= \left| \vec{X}_\delta - \vec{A}_3\vec{D}_\delta \right| \\ \vec{X}(t+1) &= \frac{\vec{X}_1 + \vec{X}_2 + \vec{X}_3}{3} \end{aligned} \tag{26}$$

Figure 8 shows a flowchart of the GWO optimization process. The approach of GWO begins with initializing a population of agents. The corresponding fitness function is calculated, and the wolves' positions are updated via updating the vectors X_α, X_β, and X_δ. The fitness function due to the updated

positions is calculated, and the presented constraints are investigated. The process is continued until the optimal solution is found.

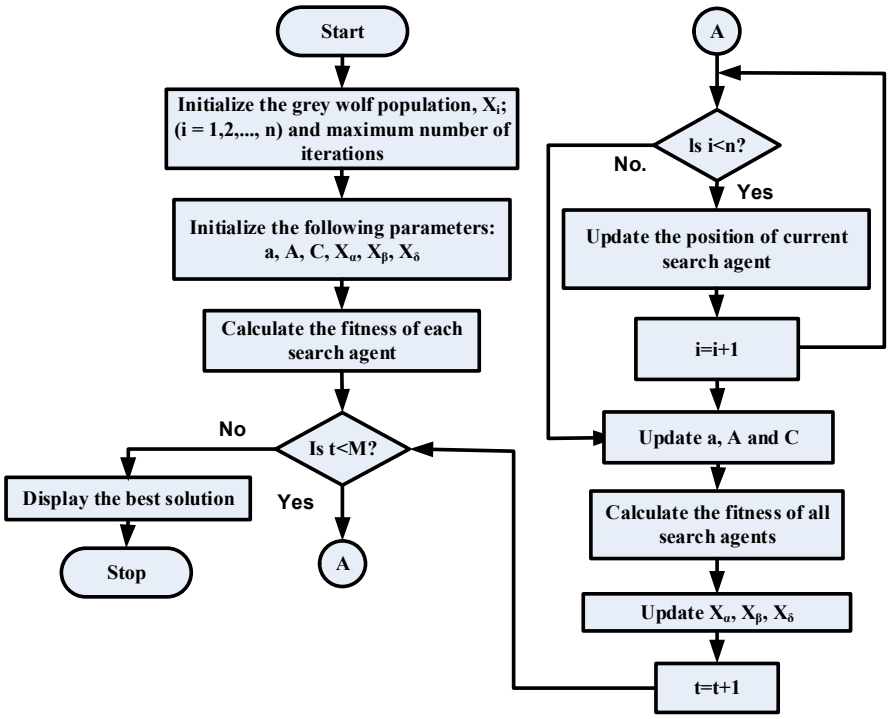

Figure 8. Flowchart of the grey wolf optimizer (GWO) process.

4. Results and Discussions

The analysis in this work was based on a square wind farm with 100 possible locations for wind turbines (10 × 10). Each WT was positioned in the center of a cell. Each cell had the dimension 200 m, which was five times the rotor diameter (5D), as shown in Figure 9. The selection of the cell dimension, equal to 5D, was to prevent the wake effect between turbines in one column with others in the adjacent columns. Additionally, it achieved the rule of thumb of the required spacing in both horizontal and vertical directions.

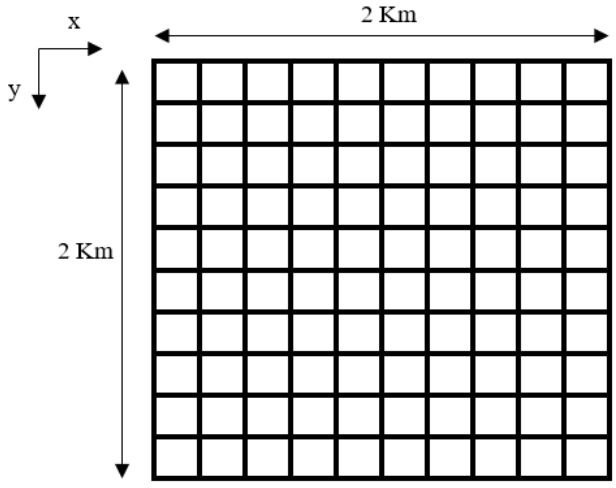

Figure 9. WF topology.

The main objective was to optimize the placement of WTs inside the WF in order to minimize the total cost per kilowatt. Two cases were studied: the first assumed constant wind speed with variable wind direction, while the second applied variable wind speed with variable wind direction. The WF used in this study had specifications tabulated in Table 2. The site ground roughness z_0 was assumed to be 0.3 m.

Table 2. Specifications of WF.

Parameter	Value
Hub height (z)	60 m
Rotor radius (r_0)	20 m
Thrust coefficient	0.88
WF area	2 Km × 2 Km
Air density	1.2254 kg/m^3
Rotor efficiency	0.4

The proposed approach incorporating WCA was applied to both cases, and the results were compared with other reported methods. This included methods proposed by Grady [11], Mosetti [27], and Feng [19] as well as other programmed approaches, namely, DE, GWO, SSA, and SBO. All approaches were simulated with a population size of 200 and a maximum iteration of 100. The lower and upper bounds were set as 0 and 1, respectively, while the dimension of the problem was 100. In the first studied case, a constant wind speed of 12 m/s was considered with equal probability of wind flow from any direction. This was done by considering 36 angles from 0° to 360° in steps of 10°. The presented WCA was applied in this case, and the optimal solution is tabulated and compared with other reported and programmed approaches in Table 3. The optimal configuration of wind farm obtained via WCA in comparison with those obtained by Grady [11] and Mosetti [27] is given in Figure 10. Referring to Table 3, it can be seen that the best solution was obtained from the proposed approach incorporating WCA. This approach gave annual power of 17,878.32 kW obtained from 40 turbines, with a total cost of $1.538/W and efficiency of 86.22%. The second best solution was obtained via DE. Figure 11 shows the time responses of the programmed approaches compared with WCA. As can be seen, the response of WCA was the best one compared to the others. Bar charts of the optimal WCA solution and the other programmed approaches are given in Figure 12. The obtained results confirmed the superiority of WCA in optimally configuring the wind farm.

Table 3. Optimal solution obtained in the case of constant wind speed with variable wind direction (CSVD).

Method	Number of Turbines	P_t (kW Year)	Cost/W ($)	Efficiency (%)
Grady [11]	39	17,220	1.567	85.174
Mosetti [27]	19	9244	1.736	NA
Feng (1) [19]	39	17,406	1.547	NA
DE	40	17,877	1.538	86
GWO	40	17,817	1.543	86
SSA	39	17,175	1.567	85
SBO	40	17,254	1.593	83
WCA	40	17,878.32	1.538	86.22

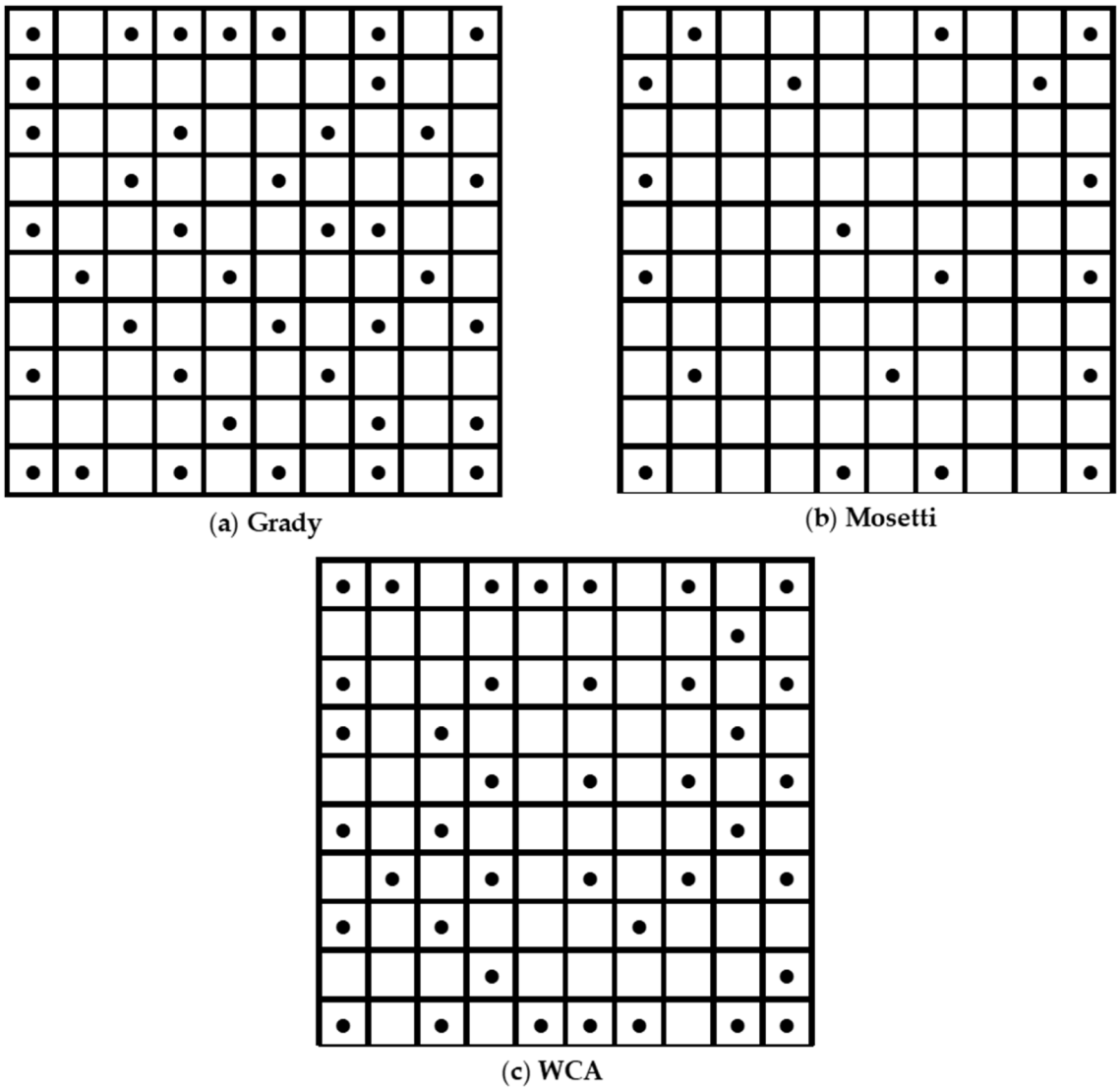

Figure 10. Optimal wind farm configuration for CSVD.

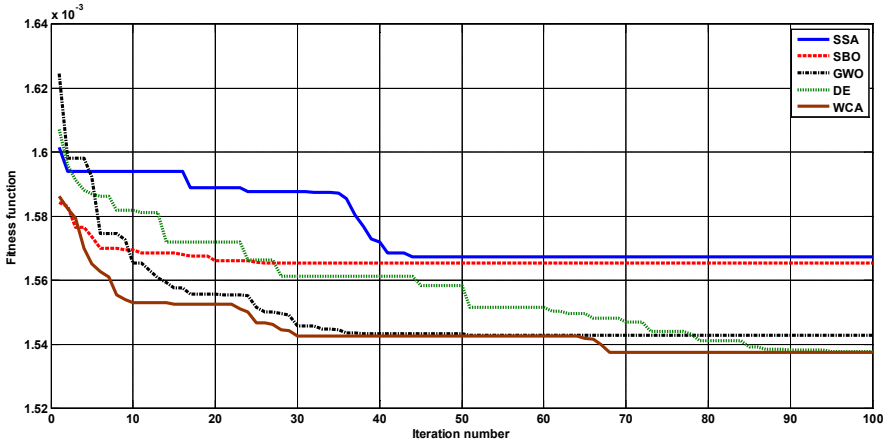

Figure 11. Time responses of different programmed approaches for CSVD.

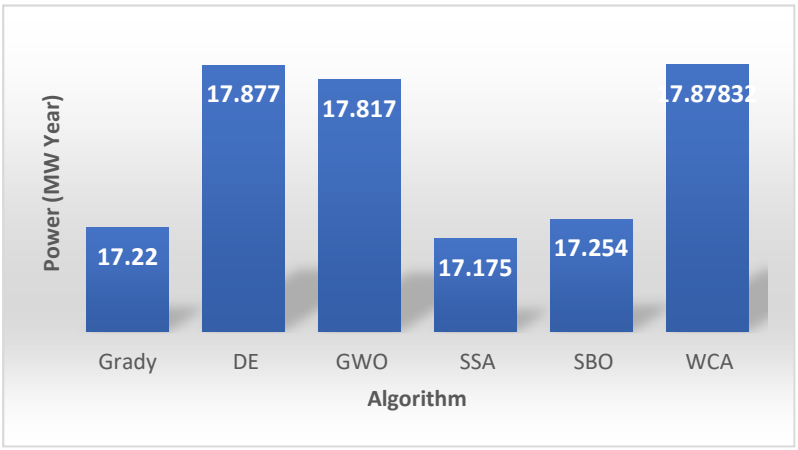

(**a**)

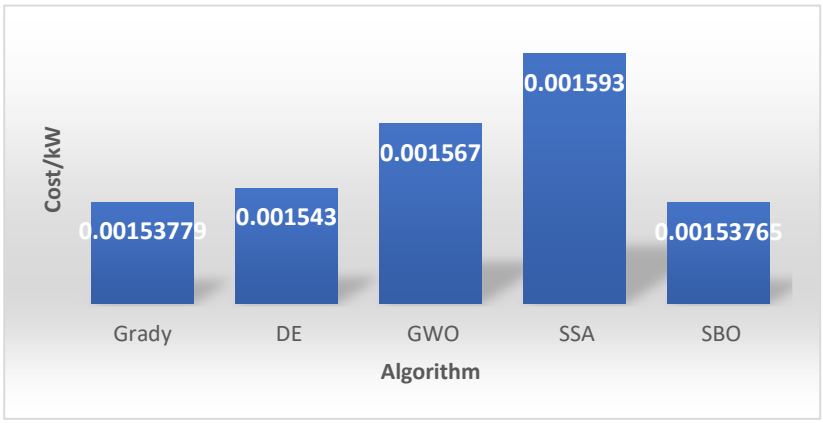

(**b**)

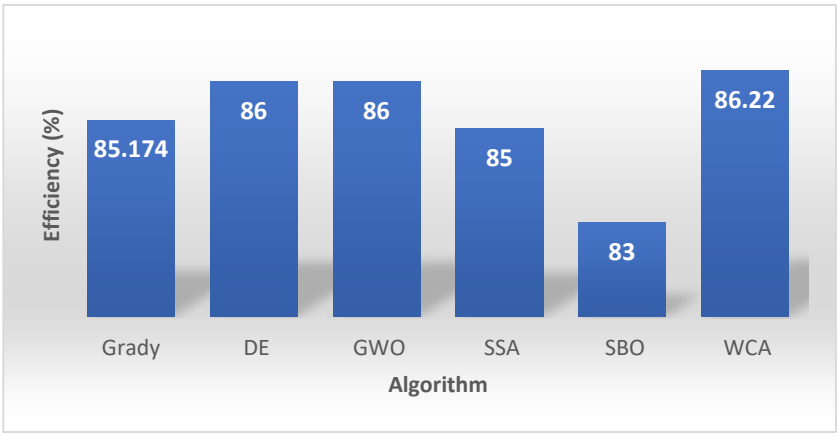

(**c**)

Figure 12. Bar chart of the optimal solutions for constant CSVD: (**a**) total power (MW/year), (**b**) cost per kW ($), and (**c**) efficiency (%).

To confirm the validity of the proposed methodology in optimally configuring the wind farm, variable wind speed with variable wind direction was considered. In this case, three wind speeds were considered—8, 12, and 17 m/s—with 36 directions in steps of 10° [1,2]. The proposed WCA was performed, and the results are tabulated and compared with reported and programmed approaches in Table 4. Referring to Table 4, it can be seen that the proposed WCA gave the best optimal solution

by configuring 40 turbines with annual cost per watt of 0.832 and total extracted annual power of 330,055 kW. The optimal configuration of the wind farm obtained with WCA in comparison to Grady and Mosetti are illustrated in Figure 13. Figure 14 displays the time responses of the proposed approach and the programmed approaches of DE, SSA, SBO, and GWO. It is clear that the response of the proposed WCA was the best compared to the others. Bar charts of the annual power, cost per watt, and efficiency of the presented approaches compared to WCA are given in Figure 15.

Table 4. Optimal solution obtained in the case of variable wind speed with variable wind direction (VSVD).

Method	Number of Turbines	P_t (kW Year)	Cost/W ($)	Efficiency (%)
Grady [11]	39	31,850	0.840	86.619
Mosetti [27]	15	13,460	0.994	NA
Feng (1) [19]	39	32,096	0.839	NA
DE	40	32,901.41	0.836	86
GWO	38	31,498	0.837	86
SSA	41	33,099	0.848	85
SBO	40	32,501.28	0.846	85
WCA	40	33,005	0.833	87

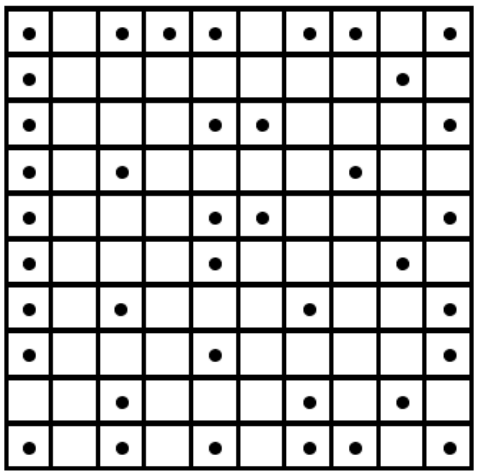

(b) Grady

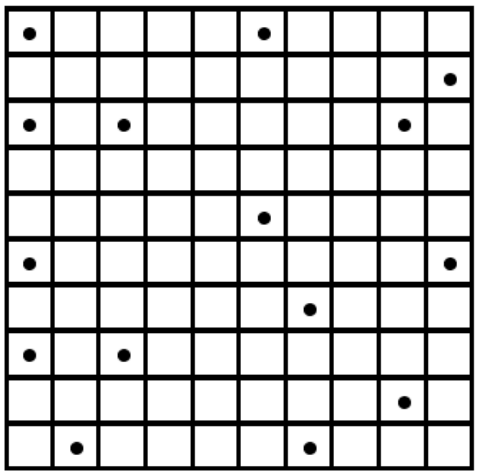

(b) Mosetti

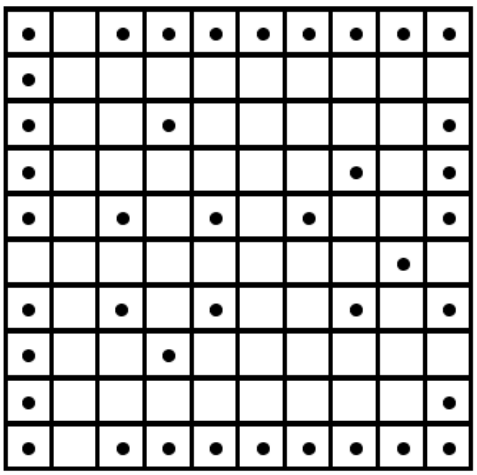

(c) WCA

Figure 13. Optimal wind farm configuration for VSVD.

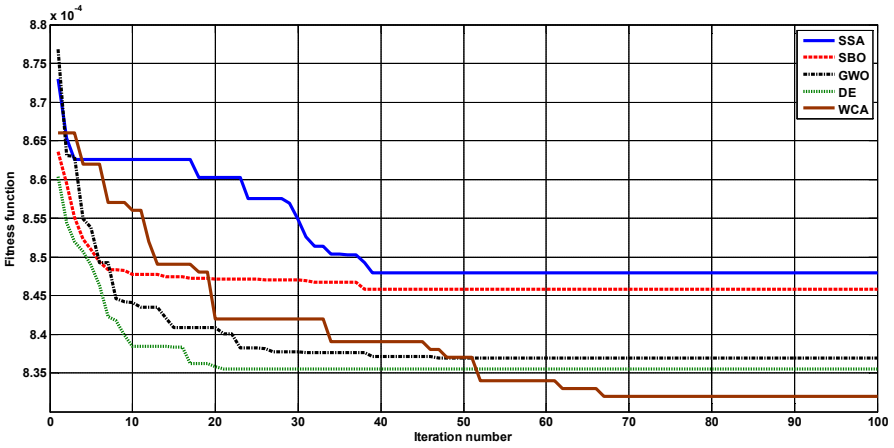

Figure 14. Time responses of programmed approaches for VSVD.

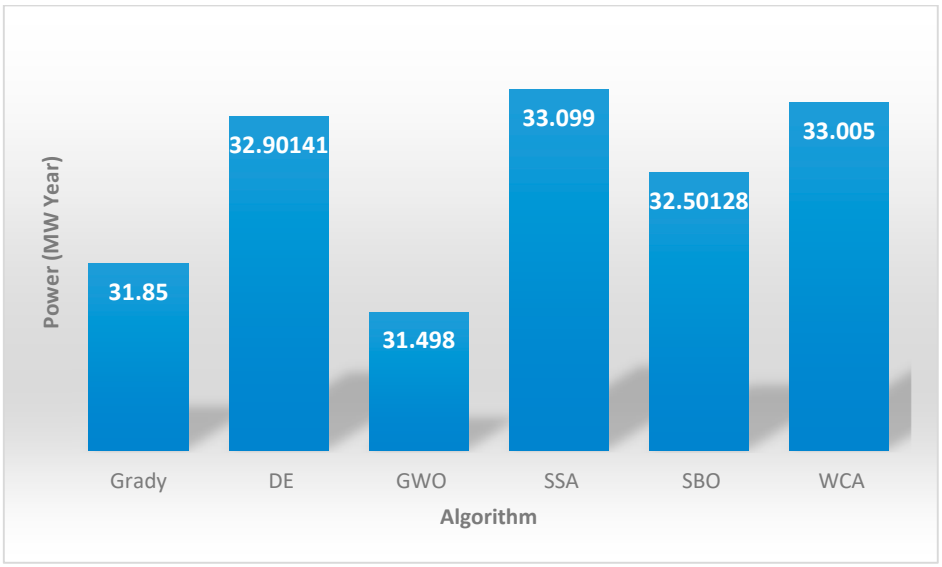

(**a**)

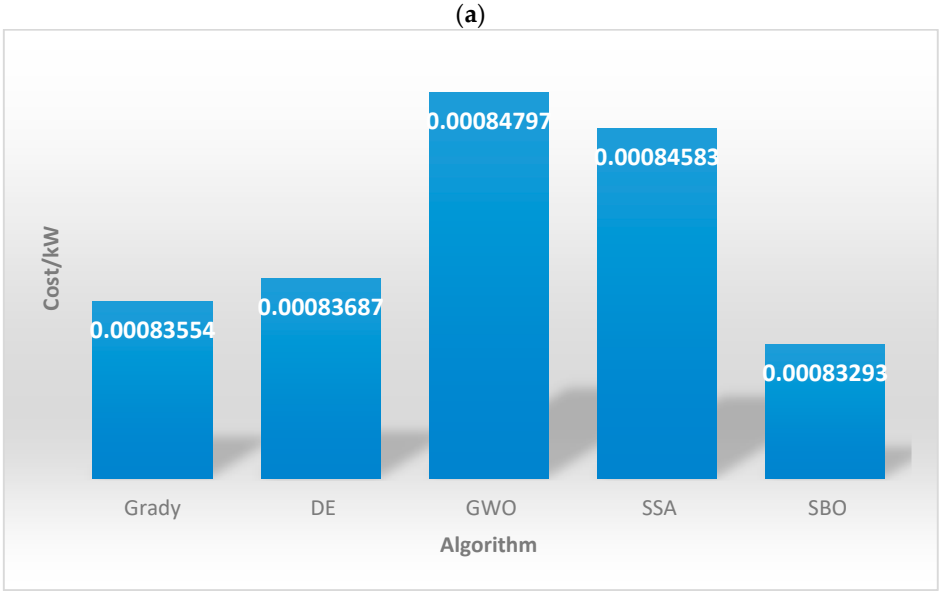

(**b**)

Figure 15. *Cont.*

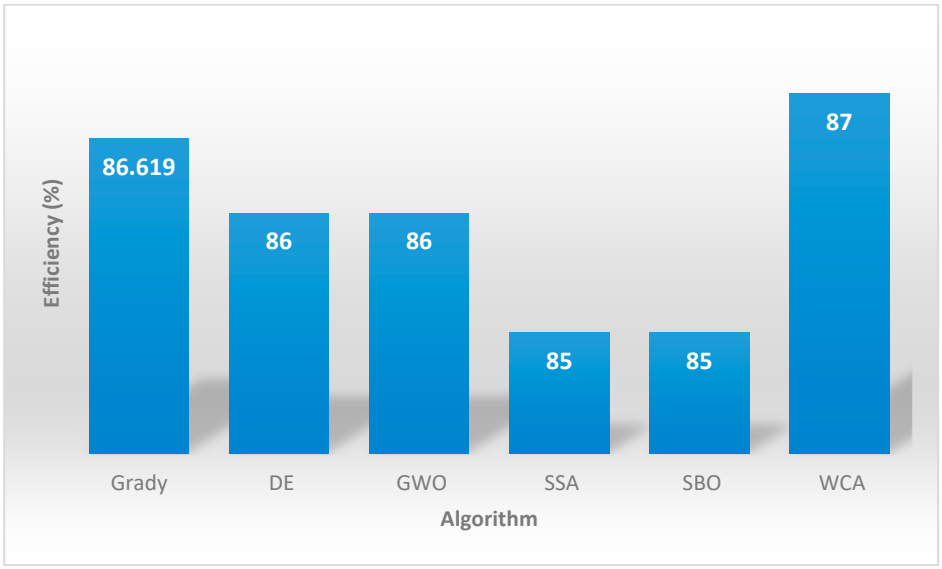

(**c**)

Figure 15. Bar chart of the optimal solutions for VSVD: (**a**) total power (MW/year), (**b**) cost per kW ($), and (**c**) efficiency (%).

Finally, the obtained results confirmed the reliability and validity of the proposed WCA in optimally configuring turbines in a wind farm for both the studied cases as the algorithm gave the best solution compared to other reported and programmed algorithms.

5. Conclusions

The optimal placement of wind turbines was determined using the recently developed water cycle algorithm. Minimization of the total cost per kilowatt was selected as the objective function during the optimization process, while the decision variables were represented by the wind turbine position and the generated output power. Two different cases were considered: (1) fixed speed and variable wind direction and (2) variable speed and variable wind direction. The results were compared with those obtained by SSA, SBO, GWO, DE, and other reported works. In the first case, the presented WCA succeeded in extracting total annual power of 17,878.32 kW with total annual cost per watt of $1.53765 and efficiency of 86.22%. This confirmed WCA to be the best optimizer compared to other reported approaches, followed by DE. In the second case, the WCA again gave the best optimal solution, with total annual power of 33,005 kW, total cost per watt of $0.833, and efficiency of 87%. A comparison of the different methods confirmed that the WCA-based optimal placement of WTs was the best among other considered methods. Advanced methods to estimate aerodynamic wake, such as modeling with computational fluid dynamic tools, should be considered in future work.

Author Contributions: Conceptualization, A.A.Z.D., A.F. and H.R.; methodology, A.A.Z.D., A.F. and H.R.; software, A.A.Z.D., A.F. and M.A.-D.; formal analysis, A.F. and H.R.; investigation, A.A.Z.D., and H.R.; resources, A.A.Z.D., A.F. and H.R.; writing—original draft preparation, A.A.Z.D., A.F., M.A.-D. and H.R.; writing—review and editing, A.A.Z.D., A.F., M.A.-D. and H.R.

Funding: This research received no external funding.

Conflicts of Interest: The authors confirm no conflicts of interest.

References

1. Marmoush, M.M.; Rezk, H.; Shehata, N.; Henry, J.; Gomaa, M.R. A novel merging Tubular Daylight Device with Solar Water Heater–Experimental study. *Renew. Energy* **2018**, *125*, 947–961. [CrossRef]
2. Rezk, H.; El-Sayed, A.M. Sizing of a stand-alone concentrated photovoltaic system in Egyptian site. *Electrical Power Energy Syst.* **2013**, *45*, 325–330. [CrossRef]

3. Rezk, H. A comprehensive sizing methodology for stand-alone battery-less photovoltaic water pumping system under the Egyptian climate. *J. Cogent Eng.* **2016**, *3*. [CrossRef]
4. Rezk, H.; Dousoky, G.M. Technical and economic analysis of different configurations of stand-alone hybrid renewable power systems—A case study. *Renew. Sustain. Energy Rev.* **2016**, *62*, 941–953. [CrossRef]
5. Hemeida, M.G.; Rezk, H.; Hamada, M.M. A comprehensive comparison of STATCOM versus SVC-based fuzzy controller for stability improvement of wind farm connected to multi-machine power system. *Electr. Eng.* **2018**, *100*, 935–951. [CrossRef]
6. Renewables 2018 Global Status Report. Available online: http://www.ren21.net/status-of-renewables/global-status-report/ (accessed on 2 November 2018).
7. Bastankhah, M.; Porté-Agel, F. A new analytical model for wind-turbine wakes. *Renew. Energy* **2014**, *70*, 116–123. [CrossRef]
8. Khanali, M.; Ahmadzadegan, S.; Omid, M.; Nasab, F.K.; Chau, K.W. Optimizing layout of wind farm turbines using genetic algorithms in Tehran province, Iran. *Int. J. Energy Environ. Eng.* **2018**, *9*, 399–411. [CrossRef]
9. Biswas, P.P.; Suganthan, P.N.; Amaratunga, G.A.J. Optimization of Wind Turbine Rotor Diameters and Hub Heights in a Windfarm Using Differential Evolution Algorithm. In *Proceedings of Sixth International Conference on Soft Computing for Problem Solving*; Advances in Intelligent Systems and Computing; Springer: Singapore, 2017; Volume 547.
10. DuPont, B.; Cagan, J.; Moriarty, P. An advanced modeling system for optimization of wind farm layout and wind turbine sizing using a multi-level extended pattern search algorithm. *Energy* **2016**, *106*, 802–814. [CrossRef]
11. Grady, S.A.; Hussaini, M.Y.; Abdullah, M.M. Placement of wind turbines using genetic algorithms. *Renew. Energy* **2005**, *30*, 259–270. [CrossRef]
12. Emami, A.; Noghreh, P. New approach on optimization in placement of wind turbines within wind farm by genetic algorithms. *Renew. Energy* **2011**, *35*, 1559–1564. [CrossRef]
13. Chen, Y.; Li, H.; Jin, K.; Song, Q. Wind farm layout optimization using genetic algorithm with different hub height wind turbines. *Energy Convers. Manag.* **2013**, *70*, 56–65. [CrossRef]
14. Shakoor, R.; Hassan, M.Y.; Raheem, A.; Rasheed, N.; Mohd, N. Wind farm layout optimization by using Definite Point selection and genetic algorithm. In Proceedings of the 2014 IEEE International Conference on Power and Energy (PECon), Kuching, Malaysia, 1–3 December 2014; pp. 191–195.
15. Turner, S.D.O.; Romero, D.A.; Zhang, P.Y.; Amon, C.H.; Chan, T.C.Y. A new mathematical programming approach to optimize wind farm layouts. *Renew. Energy* **2004**, *63*, 674–680. [CrossRef]
16. Gao, X.; Yang, H.; Lin, L.; Koo, P. Wind turbine layout optimization using multi-population genetic algorithm and a case study in Hong Kong offshore. *J. Wind Eng. Ind. Aerodyn.* **2015**, *139*, 89–99. [CrossRef]
17. Eroğlu, Y.; Seçkiner, S.U. Design of wind farm layout using ant colony algorithm. *Renew. Energy* **2012**, *44*, 53–62. [CrossRef]
18. Chowdhury, S.; Zhang, J.; Messac, A.; Castillo, L. Unrestricted wind farm layout optimization (UWFLO): Investigating key factors influencing the maximum power generation. *Renew. Energy* **2012**, *38*, 16–30. [CrossRef]
19. Feng, J.; Shen, W.Z. Solving the wind farm layout optimization problem using random search algorithm. *Renew. Energy* **2015**, *78*, 182–192. [CrossRef]
20. Marmidis, G.; Lazarou, S.; Pyrgioti, E. Optimal placement of wind turbines in a wind park using Monte Carlo simulation. *Renew. Energy* **2008**, *33*, 1455–1460. [CrossRef]
21. Mora, J.C.; Barón, J.M.C.; Santos, J.M.R.; Payán, M.B. An evolutive algorithm for wind farm optimal design. *Neurocomputing* **2007**, *70*, 2651–2658. [CrossRef]
22. Wolpert, D.H.; Macready, W.G. No free lunch theorems for optimization. *IEEE Trans. Evol. Comput.* **1997**, *1*, 67–82. [CrossRef]
23. Tolba, M.; Rezk, H.; Diab, A.; Al-Dhaifallah, M. A Novel Robust Methodology Based Salp Swarm Algorithm for Allocation and Capacity of Renewable Distributed Generators on Distribution Grids. *Energies* **2018**, *11*, 2556. [CrossRef]
24. Eskandar, H.; Sadollah, A.; Bahreininejad, A.; Hamdi, M. Water cycle algorithm—A novel metaheuristic optimization method for solving constrained engineering optimization problems. *Comput. Struct.* **2012**, *110*, 151–166. [CrossRef]

25. Mirjalili, S.; Gandomi, A.; Mirjalili, S.Z.; Saremi, S.; Faris, H.; Mirjalili, S.M. Salp Swarm Algorithm: A bio-inspired optimizer for engineering design problems. *Adv. Eng. Softw. J.* **2017**, *114*, 163–191. [CrossRef]
26. Hamid, S.S.M.; Khatibi, V.B. Satin bowerbird optimizer: A new optimization algorithm to optimize ANFIS for software development effort estimation. *Eng. Appl. Artif. Intell.* **2017**, *60*, 1–15. [CrossRef]
27. Mosetti, G.; Poloni, C.; Diviacco, B. Optimization of wind turbine positioning in large wind farms by means of a genetic algorithm. *J. Wind Eng. Ind. Aerodyn.* **1994**, *51*, 105–116. [CrossRef]
28. Rezk, H.; Fathy, A. A novel optimal parameters identification of triple-junction solar cell based on a recently meta-heuristic water cycle algorithm. *Sol. Energy* **2017**, *157*, 778–791. [CrossRef]
29. Mohamed, M.A.; Diab, A.A.Z.; Rezk, H. Partial shading mitigation of PV systems via different meta-heuristic techniques. *Renew. Energy* **2018**, *130*, 1159–1175. [CrossRef]
30. Chintam, J.R.; Daniel, M. Real-Power Rescheduling of Generators for Congestion Management Using a Novel Satin Bowerbird Optimization Algorithm. *Energies* **2018**, *11*, 183. [CrossRef]
31. Li, Q.; Chen, H.; Huang, H.; Zhao, X.; Cai, Z.; Tong, C.; Liu, W.; Tian, X. An enhanced grey wolf optimization based feature selection wrapped kernel extreme learning machine for medical diagnosis. *Comput. Math. Methods Med.* **2017**. [CrossRef]
32. Zaki Diab, A.A.Z.; Rezk, H. Optimal Sizing and Placement of Capacitors in Radial Distribution Systems Based on Grey Wolf, Dragonfly and Moth–Flame Optimization Algorithms. *Iran. J. Sci. Technol. Trans. Electr. Eng.* **2019**, *43*, 77–96. [CrossRef]